DOI 10.1007/s10891-023-02726-9
Journal of Engineering Physics and Thermophysics, Vol. 96, No. 3, May, 2023

TRANSFER PROCESSES IN RHEOLOGICAL MEDIA

CHARACTERISTICS OF VISCOPLASTIC FLUID FLOW AT VARIOUS HEAT TRANSFER REGIMES ON THE WALLS OF A SUDDEN CONTRACTION CHANNEL

K. E. Ryl′tseva and G. R. Shrager UDC 532.555.2

Consideration is given to the problem of laminar axisymmetric flow of viscoplastic fluid in a channel with a sudden cross-sectional contraction under the conditions of a variable ambient temperature. A mathematical process model is presented that includes a vortex transfer equation, the Poisson equation for the stream function, and the energy equation with account for viscous dissipation. To describe the rheological properties of a fluid, use is made of a modified Schwedoff–Bingham model within whose framework account is taken of the dependence of apparent viscosity on temperature. In the course of solving the problem, the false transient method and the numerical finite difference methodology were employed. Two heat transfer regimes on the channel walls are investigated: in the first case, a constant temperature value is assigned over the entire length of the wall, and, in the second case, a constant temperature is assigned on the walls in the vicinity of the inlet and outlet, and in the vicinity of the contraction plane, zero heat flux is assessed. The influence of thermal conditions on the structure of the flow and local pressure losses are assessed. The results of calculations in the form of distributions of flow characteristics as a function of the basic parameters of the problem are provided.

Keywords: *numerical simulation, channel contraction plane, viscoplastic medium, flow, viscous dissipation, boundary conditions, local resistance, unyielded region.*

Introduction. A fluid medium that simultaneously possesses plastic and viscous properties, a viscoplastic (structured) fluid, was first studied in detail and described by the American chemist Eugene Bingham [1]. The distinctive feature of this fluid consists in the fact that, for initiating its flow, it is required that a certain finite stress known as yield stress be applied [2]. Thus, depending on the level of stress, the viscoplastic fluid flow can be roughly divided into unyielded regions, i.e., regions where the stress is below the yield stress, and yielded flow regions, i.e., regions where the stress is equal to and higher than the yield stress. Paint-and-varnish coatings, paste- and gel-like substances and also emulsions and suspensions, the most wide-spread examples of structured fluids. For a description of rheological properties of such media, the most frequent use is made of the Bulkley–Herschel [3] or Schwedoff–Bingham models [1, 4].

The use of viscoplastic fluids in everyday life and various industries requires a detailed investigation into the characteristic features of their flow in channels of various configurations [5]. An analytical model of viscoplastic fluid flow in a flat channel was presented in [6]. The authors emphasize that in some cases, in the process of viscoplastic flow, it is necessary to use the Navier slip condition instead of the traditional no-slip condition on the walls of the channel. An alternative method of solving the problem on viscoplastic fluid flow in a thin layer with deformable walls is offered in [7]. This method makes it possible to determine all characteristics of the considered process, including the flow velocity, the pressure field, the unyielded region boundaries, the flow rate, the pressure drop, etc. A numerical investigation of viscoplastic fluid flow in an eccentric annulus and a square section channel is performed in [8]. It shows the influence of the main problem parameters on the velocity distribution in the flow whose unyielded region parameters are assessed. The conditions of a laminar-turbulent transition in viscoplastic fluid flow in a round pipe are described in [9].

Tomsk State University, 36 Lenin Ave., Bldg. 10, Tomsk, 634050, Russia; email: kiraworkst@gmail.com; shg@ftf.tsu.ru. Translated from Inzhenerno-Fizicheskii Zhurnal, Vol. 96, No. 3, pp. 652–662, May–June, 2023. Original article submitted February 5, 2022.

In considering viscoplastic fluid flow in channels of a more complex geometry, for example, in channels with sudden contraction and/or expansion, regions of low rates of strain, dead zones, were identified in the flow structure in the vicinity of the inner angles. The formation of such zones can cause a reduction in the productivity of industrial experiment or result in its breakdown. Therefore, in the course of investigations of the viscoplastic fluid flow structure, the shape and length of dead zones are analyzed [10, 11].

Yet another factor of practical significance that invites attention in considering flows in channels with a geometric feature in the form of contraction or expansion is local pressure losses. A numerical solution of the problem on viscoplastic fluid flow in plane and axisymmetric channels with a sudden expansion is presented in [12], where the dependences of local pressure losses on the problem parameters are cited along with the flow structures. The criterial dependences of the coefficient of local hydraulic resistance on the parameters of viscous plasticity and the Reynolds number for Bingham fluid flow through an axisymmetric contraction or expansion are provided in [13].

Despite most of real technological processes occurring under the conditions of variable temperature, the number of investigations devoted to nonisothermal flows of viscoplastic medium in channels of variable cross section is limited and insufficient for obtaining exhaustive information on kinematic and dynamic characteristics of the processes. Furthermore, there are almost no works that would investigate Bingham plastic flow in various thermal conditions [14].

The purpose of this work is a numerical solution of a problem of nonisothermal flow of a viscoplastic fluid through a sudden channel contraction at various regimes of heat transfer on a solid wall of the flow region.

Problem Formulation. The object of investigation represents a steady laminar flow of incompressible viscoplastic fluid in an axisymmetric channel with a sudden contraction in nonisothermal conditions with account for viscous dissipation and temperature dependence of the fluid′s viscous properties. The flow region and the notations of its characteristic dimensions are shown in Fig. 1.

For a mathematical description of the process, use is made of an equation in the stream function (ψ)–vorticity (ω)–temperature (θ) variables written in a dimensionless form [15, 16]:

$$\frac{\partial(v\omega)}{\partial r} + \frac{\partial(u\omega)}{\partial z} = \frac{2B}{\mathrm{Re}}\left(\Delta\omega - \frac{\omega}{r^2}\right) + \frac{2S}{\mathrm{Re}}\,, \tag{1}$$

$$\Delta\psi - \frac{2}{r}\frac{\partial\psi}{\partial r} = -r\omega\,, \tag{2}$$

$$\frac{\partial(v\theta)}{\partial r} + \frac{\partial(u\theta)}{\partial z} + \frac{v\theta}{r} = \frac{2}{\mathrm{Pe}}\,(\Delta\theta + A^2 B\,\mathrm{Br})\,, \tag{3}$$

where

$$S = 2\frac{\partial^2 B}{\partial r\partial z}\left(\frac{\partial v}{\partial r} - \frac{\partial u}{\partial z}\right) + 2\frac{\partial B}{\partial r}\frac{\partial\omega}{\partial r} + 2\frac{\partial B}{\partial z}\frac{\partial\omega}{\partial z} + \left(\frac{\partial^2 B}{\partial z^2} - \frac{\partial^2 B}{\partial r^2}\right)\left(\frac{\partial v}{\partial z} + \frac{\partial u}{\partial r}\right) + \frac{\partial B}{\partial r}\frac{\omega}{r}\,,$$

$$A = \left[2\left(\frac{\partial u}{\partial z}\right)^2 + 2\left(\frac{\partial v}{\partial r}\right)^2 + 2\left(\frac{v}{r}\right)^2 + \left(\frac{\partial u}{\partial r} + \frac{\partial v}{\partial z}\right)^2\right]^{1/2}.$$

The main variables are determined in the following way:

$$v = -\frac{1}{r}\frac{\partial\psi}{\partial z}\,,\quad u = \frac{1}{r}\frac{\partial\psi}{\partial r}\,,\quad \omega = \frac{\partial v}{\partial z} - \frac{\partial u}{\partial r}\,,\quad \theta = \beta_2(T - T_1)\,,$$

where T and T_1 are dimensional temperatures of the fluid in the flow and on the wall respectively.

The rheological properties of the medium are determined by the Schwedoff–Bingham law [1, 4] within whose framework the dimensionless apparent viscosity of the fluid is assigned by a formula accounting, in this case, for exponential temperature dependence [17]:

$$B = (0.5\mathrm{Bn}\,\exp(-\beta\theta) + A\,\exp(-\theta))/A\,. \tag{4}$$

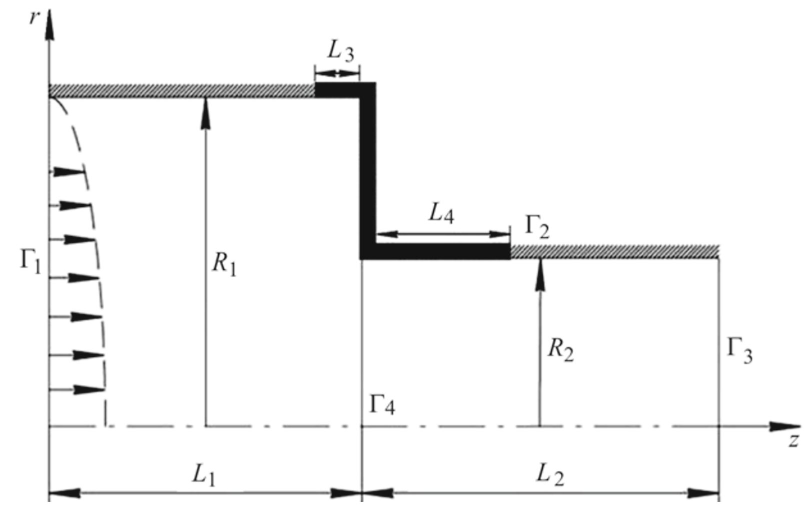

Fig. 1. Axisymmetric channel with a sudden contraction.

The dimensionless Reynolds, Peclet, Brinkman, and Bingham numbers are determined by the formulas:

$$\mathrm{Re} = \frac{2\rho U R_2}{\mu_1}, \quad \mathrm{Pe} = \frac{2c\rho U R_2}{\lambda}, \quad \mathrm{Br} = \frac{U^2 \mu_1 \beta_2}{\lambda}, \quad \mathrm{Bn} = \frac{2\tau_1 R_2}{U \mu_1}.$$

Here, the average flow rate of the fluid in the narrow portion of the channel U is assumed as a velocity scale; the radius of the narrow portion of the channel R_2 is a determining length scale; the rheological parameter at T_1 $\mu_1 = \mu_0 \exp[-\beta_2(T_1 - T_0)]$ is used in the stress scale $U\mu_1/R_2$; the limit value at T_1 is equal to $\tau_1 = \tau_0 \exp[-\beta_1(T_1 - T_0)]$; $\beta = \beta_1/\beta_2$ is the ratio of the coefficients β_1 and β_2 in temperature dependences τ_1 and μ_1; T_0 is the reference temperature.

The fluid arrives through the inlet section Γ_1 in a channel with constant dimensionless single flow rate (Fig. 1). The velocity profile $f_1(r)$ and the temperature profile $f_2(r)$ obtained in the course of solving a one-dimensional problem of a steady nonisothermal flow of viscoplastic fluid in a pipe with the dimensionless radius $R_c = R_1/R_2$ [17] are used for assigning boundary conditions at the inlet. At the outlet boundary Γ_3, "soft" boundary conditions are fulfilled. In simulating the flow region, the boundaries Γ_1 and Γ_3 are moved away from the contraction area to ensure a steady flow regime near the said boundaries. On the solid wall Γ_2, the boundary no-slip conditions are fulfilled, with dimensionless temperature equal to zero either on the entire boundary (boundary conditions, Case I), or only on its part, while on the remaining part, in the vicinity of the contraction plane, zero heat flux is assigned (boundary conditions, Case II). Symmetry conditions are implemented on the boundary Γ_4.

The mathematical notation of boundary conditions is as follows:

$$\Gamma_1 : \psi = \int_0^r f_1(r) r\, dr, \quad \omega = -\frac{\partial (f_1(r))}{\partial r}, \quad \theta = f_2(r), \quad 0 \le r \le R_c, \quad z = 0;$$

$$\Gamma_3 : \frac{\partial \psi}{\partial z} = 0, \quad \frac{\partial \omega}{\partial z} = 0, \quad \frac{\partial \theta}{\partial z} = 0, \quad 0 \le r \le 1, \quad z = \frac{L_1}{R_2} + \frac{L_2}{R_2};$$

$$\Gamma_4 : \psi = 0, \quad \omega = 0, \quad \frac{\partial \theta}{\partial r} = 0, \quad r = 0, \quad 0 < z < \frac{L_1}{R_2} + \frac{L_2}{R_2};$$

Case I of boundary conditions (Dirichlet boundary conditions for temperature):

$$\Gamma_2 : \psi = \text{const}\,, \quad \omega = -\frac{1}{r}\frac{\partial^2 \psi}{\partial r^2}\,, \quad \theta = 0\,, \quad r = R_c\,, \quad 0 < z \le \frac{L_1}{R_2}\,;$$

$$\psi = \text{const}\,, \quad \omega = -\frac{1}{r}\frac{\partial^2 \psi}{\partial z^2}\,, \quad \theta = 0\,, \quad 1 \le r < R_c\,, \quad z = \frac{L_1}{R_2}\,;$$

$$\psi = \text{const}\,, \quad \omega = -\frac{1}{r}\frac{\partial^2 \psi}{\partial r^2}\,, \quad \theta = 0, \quad r = 1\,, \quad \frac{L_1}{R_2} < z < \frac{L_1}{R_2} + \frac{L_2}{R_2}\,;$$

Case II of boundary conditions (mixed boundary conditions for temperature)

$$\Gamma_2 : \psi = \text{const}\,, \quad \omega = -\frac{1}{r}\frac{\partial^2 \psi}{\partial r^2}\,, \quad \theta = 0\,, \quad r = R_c\,, \quad 0 < z < \frac{L_1}{R_2} - \frac{L_3}{R_2}\,;$$

$$\psi = \text{const}\,, \quad \omega = -\frac{1}{r}\frac{\partial^2 \psi}{\partial r^2}\,, \quad \frac{\partial \theta}{\partial r} = 0\,, \quad r = R_c\,, \quad \frac{L_1}{R_2} - \frac{L_3}{R_2} \le z < \frac{L_1}{R_2}\,;$$

$$\psi = \text{const}\,, \quad \omega = -\frac{1}{r}\frac{\partial^2 \psi}{\partial z^2}\,, \quad \frac{\partial \theta}{\partial z} = 0\,, \quad 1 \le r \le R_c\,, \quad z = \frac{L_1}{R_2}\,;$$

$$\psi = \text{const}\,, \quad \omega = -\frac{1}{r}\frac{\partial^2 \psi}{\partial r^2}\,, \quad \frac{\partial \theta}{\partial r} = 0\,, \quad r = 1\,, \quad \frac{L_1}{R_2} < z \le \frac{L_1}{R_2} + \frac{L_4}{R_2}\,;$$

$$\psi = \text{const}\,, \quad \omega = -\frac{1}{r}\frac{\partial^2 \psi}{\partial r^2}\,, \quad \theta = 0\,, \quad r = 1\,, \quad \frac{L_1}{R_2} + \frac{L_4}{R_2} < z < \frac{L_1}{R_2} + \frac{L_2}{R_2}\,.$$

Here, L_3/R_2 and L_4/R_2 are dimensionless lengths of horizontal wall areas in which zero heat flux is assigned (Fig. 1).

Method of Solution. A numerical solution of the set problem is implemented in the following way: at the initial stage, as a result of using the false transient method [18], the main equations (1)–(3) are complemented with summands in the form of partial derivatives of sought functions (ω, ψ, θ) in the dummy time t. At the next step, we perform discretization of differential equations by means of the finite-difference procedure on the basis of alternating directions schemes [19]. In conclusion, the obtained equations are solved by the tridiagonal matrix algorithm in a discrete form [18].

To eliminate the singularity of the "infinite" value of apparent viscosity in the Schwedoff–Bingham model in unyielded regions, use is made of the regularization procedure [20] which also makes it possible to use the method of through computation in the course of numerical solution of the problem. A modified formula for calculation of apparent viscosity will assume the form

$$B = \frac{0.5\text{Bn}\,\exp\,(-\beta\theta) + \exp\,(-\theta)(A^2 + \varepsilon^2)^{0.5}}{(A^2 + \varepsilon^2)^{0.5}}\,, \tag{5}$$

where the value of the small additional parameters of regularization ε is determined in the course of a numerical experiment ($\varepsilon = 0.0125\text{Bn}$) [21].

The results of verification of the algorithm grid convergence in Case I of boundary conditions are presented in [21]. An additional check in Case II of boundary conditions is carried out for the following set of parameters: Br = 1, Pe = 10, Bn = 6, and Re = 1 (Table 1). The maximum values of axial velocity and temperature in the contraction plane calculated on a grid sequence act as control characteristics. The obtained results confirm the convergence of the algorithm being used. The analysis of the data for implementing further calculations makes it possible to select a grid step equal to 0.025.

Calculation Results. The geometry of the flow region is determined by the following values: $R_c = 2$, the contraction ratio; $L_1/R_2 = 20$, the length of the channel′s wide portion; $L_2/R_2 = 300$, the length of the channel′s narrow portion. The lengths of the solid wall portions with assigned adiabatic conditions (Case II of boundary conditions): $L_3/R_2 = 1$ and $L_4/R_2 = 3$ (Fig. 1).

Separation of unyielded regions and dead zones in the flow of viscoplastic fluid is carried out in accordance with an inequality that represents a dimensionless analog of the criterion for identifying regions with a stress level lower than the yield stress $BA \le 0.5\text{Bn}\,\exp\,(-\beta\theta)$.

TABLE 1. Maximum Velocity and Temperature in the Contraction Plane at Various Values of the Difference Grid Step h

h (grid step)	u_{max} (contraction plane)	$\boldsymbol{\theta}_{max}$ (contraction plane)
0.1	1.41105	1.19514
0.05	1.39266	1.27060
0.025	1.38682	1.32878
0.0125	1.38462	1.36158

Figure 2 shows axial velocity distributions in variation of the Bingham and Brinkman numbers in the two considered cases of heat transfer on the channel′s solid wall. One can see that with increase in Bn and Br under the conditions of fluid flow rate constancy the axial velocity of the flow in the vicinity of the channel axis rises (Fig. 2c–f). The simultaneous increase of the selected parameters results in a rise of the maximum axial velocity in the considered flow region by several times (Fig. 2g and h). Comparing the distributions obtained in Cases I and II of boundary conditions, we can note that in the case of identical sets of parameters, we observe a difference in the axial velocity profiles in the vicinity of the contradiction plane.

As a result of comparison of temperature fields obtained at various sets of problem parameters (Fig. 3), in Case II of boundary conditions, we note the formation of a fluid heatup region along the wall downstream from the contraction plane, with this region occurring due to the absence of heat flux on this portion of the solid wall and being more explicitly manifested at higher values of the Bingham and Brinkman numbers (Fig. 3b, d, f, and h). Irrespective of the assigned boundary conditions, the increase in the parameters Bn and Br contributes to the rise in the average level of temperature in the flow region (Fig. 3g and h). It is important to emphasize that in the course of simulating the considered nonisothermal process at relatively high values of dimensionless parameters, it is necessary to ensure a length of the narrow portion of the channel sufficient for the flow achieving hydrodynamic and temperature stabilization.

Figure 4 demonstrates the flow structure made up of yielded flow regions (colored white) and unyielded regions and dead zones (colored black) [21]. We can see that with increase of the Bingham number the unyielded regions formed along the axis of the wide and narrow parts of the channel expand, and the dead zone grows in size in the region of the inner angle (Fig. 4c and d). Furthermore, in Case II of boundary conditions the unyielded region in the narrow part of the channel splits into two components. The rise of the Brinkman number results in a decrease of the width of unyielded regions (Fig. 4e and f), and in Case II of boundary conditions, the unyielded region experiences splitting, apart from a reduction in size (Fig. 4f). In the case of simultaneous increase in the Bn and Br parameters, we observe the occurrence of additional dead zones in the vicinity of the solid wall in both parts of the channel, with combination of dead zones occurring in the wide part (Fig. 4g and h).

The streamline distributions along the channel for Cases I and II of boundary conditions are presented in Fig. 5a and b respectively. In both cases, in the vicinity of inlet and outlet boundaries, the flow has a one-dimensional pattern, which is indicated by the parallel arrangement of the stream line with respect to the channel axis of symmetry, with the flow assuming a two-dimensional pattern in the vicinity of the contraction plane. The apparent difference of the flow patterns in the two considered cases consists in the flow curvature on the right of the contraction plane in Case II of boundary conditions (Fig. 5b). In this region, a change occurs in the form of boundary conditions for the temperature on the solid wall, which is also manifested on the distribution of the radial velocity in the form of an additional zone of significant values (Fig. 5d).

For a quantitative assessment of the flow structure in Cases I and II of boundary conditions, we introduce dimensionless geometric flow characteristics, viz., lengths of two-dimensional flow regions in the wide and narrow parts of the channel l_1 and l_2 (Fig. 5a) determined by the extent of the portions from the contraction plane to the cross sections in which the axial velocity on the channel axis is equal to values that differ by 1% from those obtained in the one-dimensional flow region upstream and downstream respectively. Analyzing the criterial dependences of l_1 and l_2 on the dimensionless numbers Br, Pe, Re, and Bn for Cases I and II of boundary conditions, we can draw a conclusion that a change in the boundary conditions for temperature almost does not affect the length of two-dimensional flow regions, which is indicated by the absence of qualitative and substantial quantitative differences in the two considered cases (Fig. 6).

In the process of fluid flow in a channel with a sudden cross-sectional area change, we can identify two types of losses in total pressure ΔP: losses on friction ΔP_{fr} and losses on local resistance ΔP_{loc}:

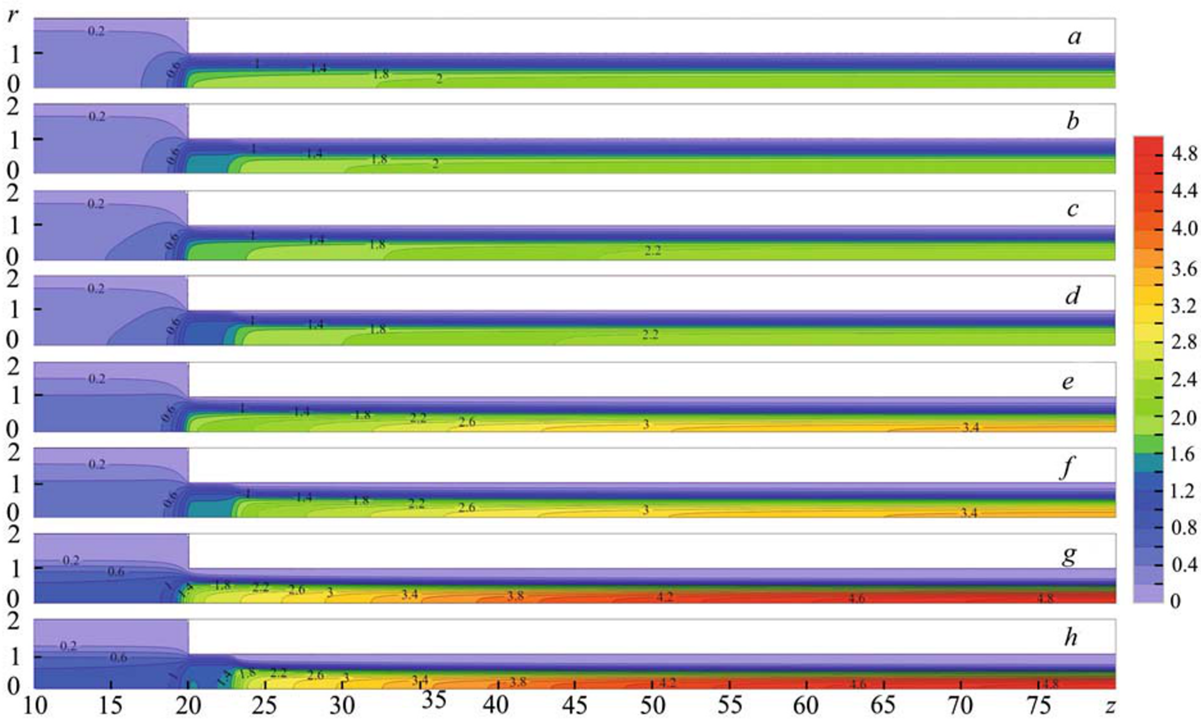

Fig. 2. Axial velocity fields at Pe = 100 and Re = 1: (a, b) Br = 1, Bn = 2; (c, d) Br = 1, Bn = 6; (e, f) Br = 4, Bn = 2; (g, h) Br = 4, Bn = 6; (a, c, e, g) Case I of boundary conditions; (b, d, f, h) Case II of boundary conditions.

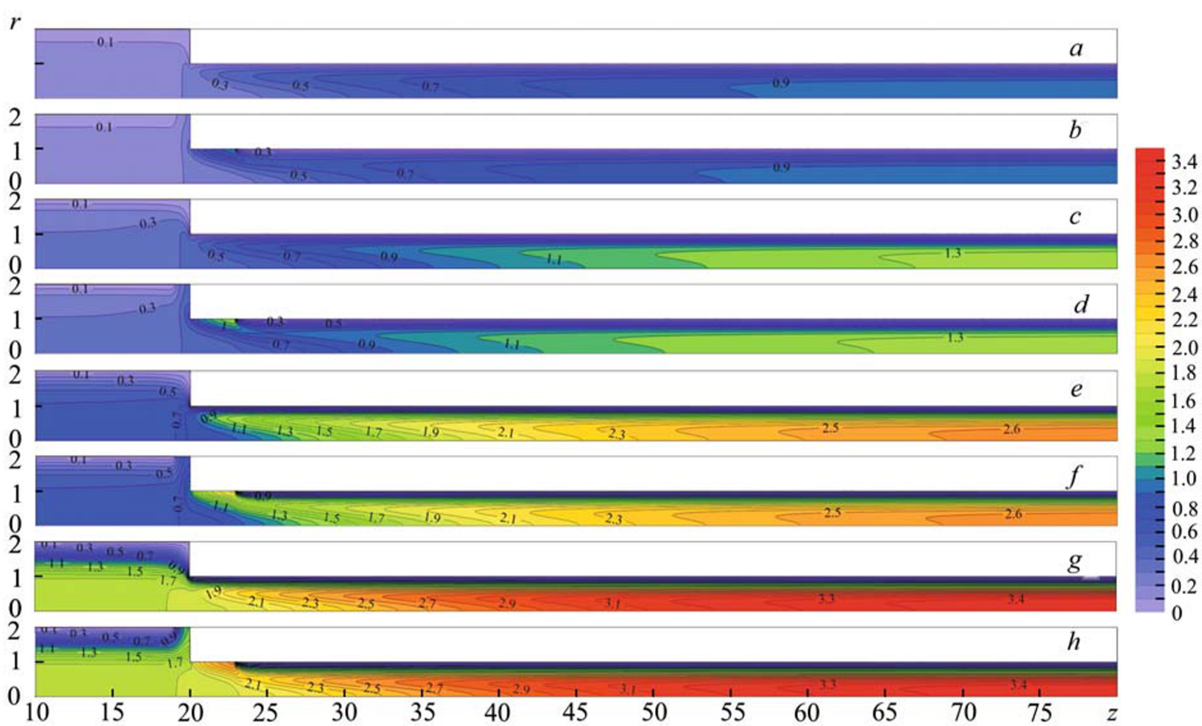

Fig. 3. Temperature fields at Pe = 100 and Re = 1: (a, b) Br = 1, Bn = 2; (c, d) Br = 1, Bn = 6; (e, f) Br = 4, Bn = 2; (g, h) Br = 4, Bn = 6; (a, c, e, g) Case I of boundary conditions; (b, d, f, h) Case II of boundary conditions.

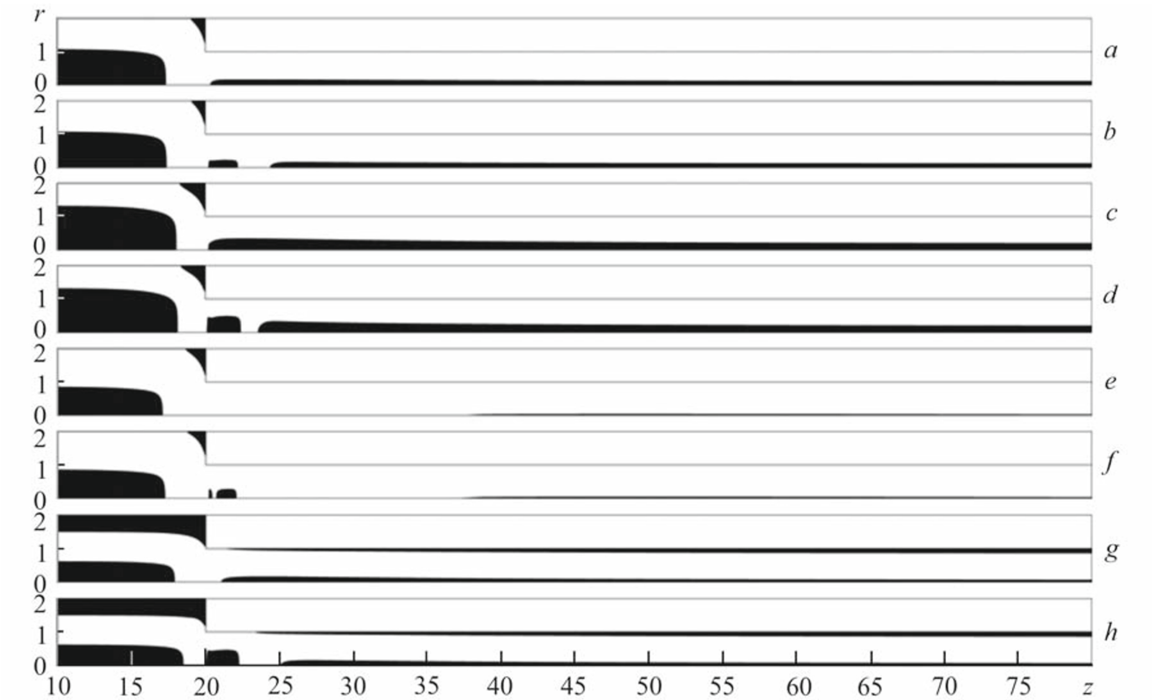

Fig. 4. Flow structure at Pe = 100 and Re = 1: (a, b) Br = 1, Bn = 2; (c, d) Br = 1, Bn = 6; (e, f) Br = 4, Bn = 2; (g, h) Br = 4, Bn = 6; (a, c, e, g) Case I of boundary conditions; (b, d, f, h) Case II of boundary conditions.

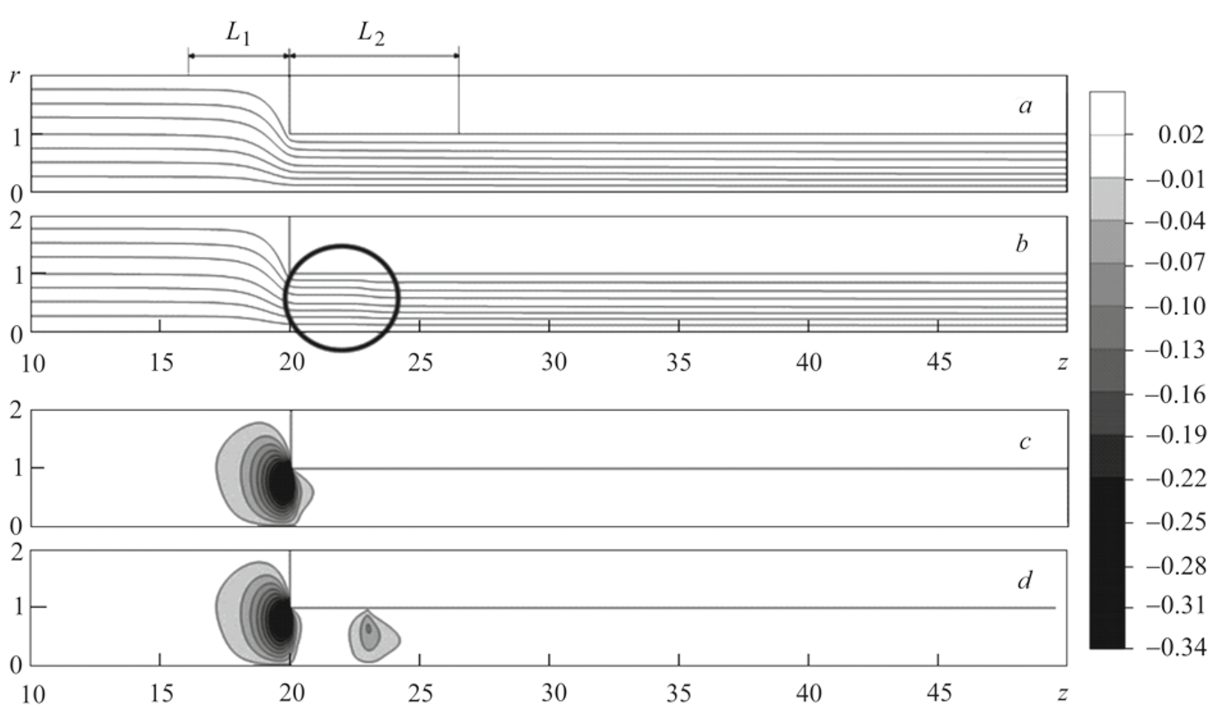

Fig. 5. Streamline distributions (a, b) and radial velocity distributions (c, d) at Br = 1, Pe = 100, Re = 1, and Bn = 2; (a, c) Case I of boundary conditions; (b, d) Case II of boundary conditions.

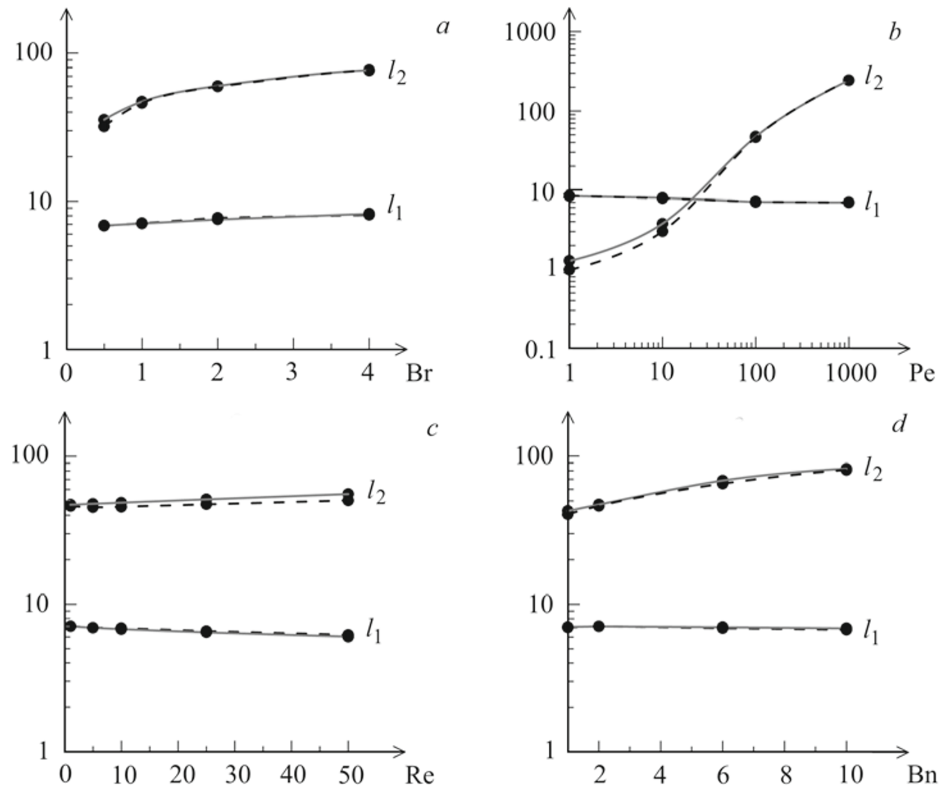

Fig. 6. Lengths of two-dimensional flow regions as a function of the Brinkman number at Pe = 100, Re = 1, and Bn = 2 (a), the Peclet number at Br = 1, Re = 1, and Bn = 2 (b), the Reynolds number at Br = 1, Pe = 100, and Bn = 2 (c), and the Bingham number at Br = 1, Pe = 100, and Re = 1 (d); solid line, Case I of boundary conditions; dashed line, Case II of boundary conditions.

$$\Delta P = \Delta P_{\text{fr}} + \Delta P_{\text{loc}} . \tag{6}$$

If we are to take the ratio of the total pressure lost in this area to the dynamic head, we will obtain a formula for calculating the resistance coefficient [22]:

$$C = \frac{\Delta P}{0.5\rho U^2} = \frac{\Delta P_{\text{fr}} + \Delta P_{\text{loc}}}{0.5\rho U^2} = C_{\text{fr}} + C_{\text{loc}} , \tag{7}$$

where C_{fr} is the friction resistance coefficient, and C_{loc} is the local resistance coefficient.

The local resistance coefficient determines quantitatively the local pressure losses that are localized in the vicinity of the contraction plane and are a consequence of an abrupt change in characteristics due to forced restructuring of the flow. The coefficient is calculated by the formula:

$$C_{\text{loc}} = \frac{\Delta p_{\text{loc}}}{(1/2)\rho U^2} + \alpha_1 \left(\frac{1}{R_{\text{c}}}\right)^4 - \alpha_2 , \tag{8}$$

where Δp_{loc} is a pressure drop characteristic of the flow transient region; the correcting coefficient for kinetic energy α_i in the wide (index 1) and narrow (index 2) parts of the channel is equal to

$$\alpha_i = \frac{1}{U^3 F_i} \int_{F_i} u_i^3 dF_i , \quad i = 1, 2 , \tag{9}$$

where F_i is the cross-sectional area of the channel.

TABLE 2. Coefficient of Local Resistance at Various Values of the Brinkman, Peclet, and Reynolds Numbers

Parameters	C_{loc}	
	Case I of boundary conditions	Case II of boundary conditions
Br = 1 (Pe = 100, Re = 1, Bn = 2)	111.340	62.845
Br = 4 (Pe = 100, Re = 1, Bn = 2)	126.327	89.632
Pe = 1000 (Br = 1, Re = 1, Bn = 2)	688.682	650.545
Re = 10 (Br = 1, Pe = 100, Bn = 2)	12.096	6.877
Bn = 10 (Br = 1, Pe = 100, Re = 1)	280.777	190.551

TABLE 3. Comparison of Values of the Local Resistance Coefficient at Various Lengths of Solid Wall Portions with Assigned Conditions of the Heat Flux Constancy at Br = 1, Pe = 100, Re = 1, and Bn = 6

Length of wall portions		C_{loc}
L_3/R_2	L_4/R_2	
1	3	114.709
2	2	129.407
3	2	115.097
2	3	98.610

For analysis of the effects of thermal conditions on the value of local pressure losses, Table 2 shows the C_{loc} values calculated at various sets of problem parameters. Calculations have shown that the value of the local resistance coefficient in Case I of boundary conditions is higher than in Case II of boundary conditions; hence, the mixed-type boundary conditions considered in this work for the temperature on the solid wall of the channel are more efficient in terms of energy losses. Furthermore, a significant decrease in C_{loc} is observed with increase in the domination of inertia forces in the flow over viscosity forces (increase in the Reynolds number).

The assessment of the influence of the length of the horizontal wall portions with an assigned Neumann boundary condition for temperature (L_3/R_2 and L_4/R_2, Fig. 1) on the local pressure losses is carried out on the basis of the data presented in Table 3. As a result of the conduct of parametric calculations, it is found that in the considered cases, the maximum value of the local resistance coefficient is achieved at $L_3/R_2 = 2$ and $L_4/R_2 = 2$, and the minimum value is reached at $L_3/R_2 = 2$ and $L_4/R_2 = 3$.

Conclusions. Numerical simulation of a viscoplastic fluid flow through a sudden contraction of a channel under nonisothermal conditions has been carried out. A series of calculations has been performed with a view to comparing the flow characteristics depending on the type of boundary conditions for temperature assigned on the solid wall of the channel. Case I of boundary conditions, Dirichlet boundary conditions are assigned across the entire wall; Case II of boundary conditions, Neumann boundary conditions are assigned on part of the wall to the left and right of the contraction plane, and Dirichlet boundary conditions are assigned on the remaining part. Axial velocity and temperature fields have been determined for the two considered cases. We have demonstrated the characteristic features of the structure of the flows that consist in the splitting of unyielded regions and the formation of additional dead zones at certain sets of parameters. We have identified qualitative dependences of the lengths of two-dimensional flow regions on the dimensionless parameters of the problem and also a substantial difference in the form of an additional region with a nonzero radial velocity in the narrow part of the channel in Case II of boundary conditions. Values of the local resistance coefficient in variation of the Brinkman, Peclet, Reynolds, and Bingham numbers have been obtained. It has been shown that the use of boundary conditions for mixed-type temperature makes it possible to reduce local pressure losses.

Acknowledgment. The investigation was carried out under a grant of the Russian Science Foundation (Project No. 18-19-00021-P).

NOTATION

A, dimensionless intensity of the rate of strain; B, dimensionless apparent fluid viscosity; Bn, Bingham number; Br, Brinkman number; c, heat capacity of a medium, J/(kg·K); C, dimensionless resistance coefficient; h, difference grid step; l_1 and l_2, dimensionless lengths of two-dimensional flow regions in the wide and narrow parts of the channel respectively; L_1/R_2 and L_2/R_2, dimensionless lengths of the wide and narrow parts of the channel respectively; L_3/R_2 and L_4/R_2, dimensionless lengths of the portions of a horizontal wall on which zero heat flux is assigned; Pe, Peclet number; Re, Reynolds number; R_1 and R_2, radii of the wide and narrow parts of the channel respectively, m; R_c, contraction ratio; S, dimensionless source term; T, temperature, K; U, average fluid flow rate in the narrow part of the channel, m/s; u and v, dimensionless axial and radial velocities along the z and r axes respectively; α, correction coefficient of kinetic energy; β_1 and β_2, coefficients in the temperature dependences τ_1 and μ_1 respectively, 1/K; Γ, flow region boundary; ΔP, total pressure losses, Pa; ε, regularization parameter; θ, dimensionless temperature; λ, heat capacity of a medium, W/(m·K); μ_1, rheological parameter at T_1, Pa·s; ρ, density of a medium, kg/m^3; τ_1, stress limit value at T_1, Pa; ψ, stream function; ω, vorticity. Subscripts: fr, friction; loc, local; max, maximum.

REFERENCES

1. E. C. Bingham, *Fluidity and Plasticity*, McGraw-Hill, New York (1922).
2. K. Walters, The yield stress concept — Then and now, *Plenary Lecture Given at the YPF 2009 Conference* (2009).
3. W. H. Herschel and R. Bulkley, Konsistenzmessungen von Gummi-Benzollosungen, *Kolloid-Zeitschrift*, **39**, 291–300 (1926).
4. T. Schwedoff, Recherches expérimentales sur la cohésion des liquids, *Journal de Physique Théorique et Appliquée*, **8**, 341–359 (1889).
5. E. Mitsoulis and J. Tsamopoulos, Numerical simulations of complex yield-stress fluid flows, *Rheol. Acta*, **56**, No. 3, 231–258 (2017).
6. A. Lawal, D. M. Kalyon, and U. Yilmazer, Extrusion and lubrication flows of viscoplastic fluids with wall slip, *Chem. Eng. Commun.*, **122**, No. 1, 127–150 (1993).
7. A. V. Gnoevoi, D. M. Klimov, A. G. Petrov, and V. M. Chesnokov, Plane viscoplastic flow in narrow channels with deformable walls, *Fluid Dyn*., **31**, No. 2, 178–185 (1996).
8. Y. Wang, Axial flow of generalized viscoplastic fluids in non-circular ducts, *Chem. Eng. Commun.*, **168**, No. 1, 13–43 (1998).
9. A. G. Potapov, Laminar-turbulent transition at flow of Newtonian and non-Newtonian fluids in a round tube, *Scientific-Technical Collection Book "Gas Science Bulletin,"* **2**, No. 26, 174–182 (2016).
10. A. N. Alexandrou, T. M. McGilvreay, and G. Burgos, Steady Herschel–Bulkley fluid flow in three-dimensional expansions, *J. Non-Newtonian Fluid Mech*., **100**, Nos. 1–3, 77–96 (2001).
11. P. Jay, A. Magnin, and J. M. Piau, Viscoplastic fluid flow through a sudden axisymmetric expansion, *AIChE J*., **47**, No. 10, 2155–2166 (2001).
12. E. Mitsoulis and R. R. Huilgol, Entry flows of Bingham plastics in expansions, *J. Non-Newtonian Fluid Mech*., **122**, Nos. 1–3, 45–54 (2004).
13. S. L. D. Kfuri, E. J. Soares, R. L. Thompson, and R. N. Siqueira, Friction coefficients for Bingham and power-law fluids in abrupt contractions and expansions, *J. Fluids Eng*., **139**, No. 2, 1–8 (2016).
14. E. J. Soares, M. F. Naccache, and P. R. Souza Mendes, Heat transfer to viscoplastic materials flowing axially through concentric annuli, *Int. J. Heat Fluid Flow*, **24**, No. 5, 762–773 (2003).
15. V. I. Yankov, I. O. Glot, N. M. Trufanova, and N. V. Shakirov, *Flow of Polymers through Spinneret Holes. Theory, Computation, and Practice* [in Russian], Regulyarnaya i Khaoticheskaya Dinamika, Moscow–Izhevsk (2010).
16. G. B. Froyshteter, S. Yu. Danilevich, and N. V. Radionova, *Flow and Heat Transfer of Non-Newtonian Fluids through Pipes* [in Russian], Naukova Dumka, Kyiv (1990).
17. E. I. Borzenko, K. E. Ryltseva, and G. R. Shrager, Non-isothermal steady flow of non-Newtonian fluid in an axisymmetric channel, *IOP Conf. Ser.: Mater. Sci. Eng.*, **58**, 1–9 (2019).

18. S. K. Godunov and V. S. Ryabenkiy, *Difference Schemes*, Elsevier Sci. Ltd, North Holland (1987).
19. A. A. Samarskiy, *Introduction to the Theory of Difference Schemes* [in Russian], Nauka, Moscow (1971).
20. M. Bercovier and M. Engelman, A finite-element method for incompressible non-Newtonian flows, *J. Comput. Phys*., **36**, 313–326 (1980).
21. K. E. Ryltseva, E. I. Borzenko, and G. R. Shrager, Non-Newtonian fluid flow through a sudden pipe contraction under non-isothermal conditions, *J. Non-Newtonian Fluid Mech.*, **286**, 1–13 (2020).
22. I. E. Idelchik, *Handbook of Hydraulic Resistance*, Israel Program for Sci. Translations, Jerusalem (1966).